August 2012

Master's Degree Thesis

Extraction of Brain Tumor Using Level Set Method with Automatic Selective Local Statistics and SPF in MR Images

Graduate School of Chosun University

Department of Information and Communication Engineering

Kiran Thapaliya

August 2012

Master's Degree Thesis

Extraction of Brain Tumor Using Level Set Method with Automatic Selective Local Statistics and SPF in MR Images

Thakpiarlaiya

Extraction of Brain Tumor Using Level Set Method with Automatic Selective Local Statistics and SPF in MR Images

MR 영상에서 SPF와 자동 선택적 지역 통계에 의한 Level set 방식을 이용한 뇌 종양 추출

August 24, 2012

Graduate School of Chosun University

Department of Information and Communication Engineering

Kiran Thapaliya

Extraction of Brain Tumor Using Level Set Method with Automatic Selective Local Statistics and SPF in MR Images

Advisor: Prof. Goo-Rak Gwon

This thesis is submitted to Chosun University in partial fulfillment of the requirements for a Master's degree

April 2012

Graduate School of Chosun University

Department of Information and Communication Engineering

Kiran Thapaliya

타팔리야 키란의 석사학위 논문을 인준함

위원장 조선대학교 교수 박 종 안 

위 원 조선대학교 교수 신 영 숙 

위 원 조선대학교 교수 권 구 락 

2012년 5월

조 선 대 학 교 대 학 원

Table of Contents

List of Tables

List of Figures

Acronyms

MRI	:	Magnetic Resonance Image
WHO	:	World Health Organization
CT	:	Computerized Tomography
CV	:	Chan-Vase
GAC	:	Geodesic Active Contour
SPF	:	Signed Pressure Function
CNS	:	Central Nervous System
AIDS	:	Acquired Immune Deficiency Syndrome
SD	:	Small Deforming Tumors
LD	:	Large Deforming Tumors
SVM	:	Support Vector Machine
MRF	:	Markov Random Field
ESF	:	Edge Stopping Function
JM	:	Jaccards Measure
DC	:	Dice Coefficient
RMSE	:	Root Mean Square Error

ABSTRACT

Extraction of Brain Tumor Using Level Set Method with Automatic Selective Local Statistics and SPF in MR Images

Kiran Thapaliya
Advisor: Prof. Goo-Rak Kwon, Ph.D
Department of Information and Communications Engineering
Graduate School of Chosun University

The level set approach can be used as a powerful tool for the segmentation of the images. The purpose of this study is to propose a method of a segmentation of brain tumor images from MR images. In this paper, we introduce a new signed pressure function (SPF) which can efficiently stop the contours at weak or blurred edges. The local statistics of the different objects present in the MR images are calculated. With the help of the local statistics, tumor objects are identified among different objects. In this level set method, the calculation of parameters is a challenging job. The calculations of different parameters for different kind of images are automatic. The basic thresholding value is updated and adjusted automatically for different MR images. This thresholding values are used to calculate the different parameters in the proposed algorithm. The proposed algorithm has been tested on magnetic resonance images of the brain for tumor segmentation and its performance evaluated visually and quantitatively. Numerical experiments on some brain tumor images have demonstrated the efficiency and robustness of our method.

I. Introduction

A tumor is an abnormal growth of body tissue. It is one of the most common brain diseases, therefore its diagnosis and treatment have a vital role for the patients to be cured from tumor. Many medical imaging techniques allow us to use them in several domain of medicine, for example, computer aided pathologies diagnosis, follow-up of these pathologies, surgical planning, surgical guidance, statistical and time series analysis. Among all these, Magnetic Resonance Imaging (MRI) is the most common used imaging technique in neuroscience and neurosurgery for these applications. Segmentation of targeted objects, mainly anatomical structures and pathologies from MR images is a fundamental task, since the results often become the basis for other applications. The segmentation of medical images is a challenging task, because they usually involve a large amount of data, they have some-times some artifacts due to patient's motion or limited acquisition time and soft tissue boundaries are usually not well define.

When the segmentation of the brain tumor has to be performed, many other problem arises which makes their segmentation more difficult. We can find a large class of tumor types which have different shapes and sizes. The location of brain tumor is not fixed and they vary in intensities.

Some terms used to describe magnetic resonance imaging techniques are listed in below table

Table 1.1 Terms used to describe MRI techniques

Term	Description
T1	The time needed for the protons within the tissue to return to their original state of magnetization
T2	The time required for the protons perturbed into coherent oscillation by the radio frequency pulse to lose this coherence
TR	Repetition time: the time between successive applications of radio frequency pulse sequences
TE	Echo time: the delay before the radio frequency energy radiated by the tissue.
T1-weighted	Short TR, short TE. Provides letter anatomic detail
T2-weighted	Long TR, short TE. More sensitive to water content and as a result, more sensitive to pathology
FLAIR image	Long TR, short TE. Improved contrast between lesions and cerebrospinal fluid.

A. Thesis Motivation and Overview

Segmentation of brain tumor from MR images is a difficult task that involves the various type of disciplines covering pathology, MRI physics, radiologist's perception, and image analysis based on intensity , shape and size. There are several issues and challenges in proper segmentation of brain tumor. According to the data of World Health Organization (WHO), more than 4,00,000 persons take the treatment of brain tumor every year. Tumor differs with it is shape, size and location, they can appear at different places with different intensities, therefore it's difficult to find the exact tumor in the brain. The accurate segmentation of brain tumors is of great interest. We can classify the brain tumor as primary tumor called beningn which do not spread elsewhere and another is called secondary or malignant brain tumor which spreads from the other location of the body to the brain. In order to find the tumor in the brain, the patients in the hospital undergoes diagnosis like CT-scan and MRI. Even though, the radiologist performs these diagnosis, it is very difficult to identify the

tumor in the brain due to the involvement of various kinds of abnormalities, noises and intensities.

B. Research Objectives

In this context, the first aim of this work is to develop a framework for a robust and accurate segmentation of large class of brain tumor in MR images. We proposed a new region based method for the segmentation of brain tumor using the advantages of CV and GAC method. This paper presents the formulation of design of signed pressure function (SPF) using the adaptive local statistics information of the object present in the magnetic resonance image. The thresholding values for the different objects in the images are adapted automatically. The main problem in level set method is the calculation of its different parameters. In [21], different parameters are tuned manually for different kinds of images during the test of the image. In the proposed method, no parameters are tuned manually; different parameters are set automatically for different kinds images.

C. Thesis Contribution

In this thesis, a new algorithm for the extraction of the brain tumor is presented. We use the level set and signed pressure function to extract the tumor part from the brain. Different parameters are calculated automatically based on the image features. Important algorithms that are proposed in the field of brain tumor segmentation are explained in this thesis. The main contributions of this thesis are as follows:

New algorithm: A new algorithm is designed for the brain tumor extraction without considering the evolution of contour in the image, and no matter whether the edge of the image is weak or blur.

Design Procedure: a design procedure is given in order to find the important parameters of this algorithm. For a given application with its specifications and requirements, an engineer can follow the steps in this procedure to find the important parameters and also the appropriate number of phases in this algorithm.

Simulation: A simulation code was written in MAT Lab 2010 to test the performance of this algorithm and compare with other algorithms.

D. Thesis Organization

The remainder of this paper is organized as follows: In section 2, we review the classic GAC and CV models. In section 3 we describe the proposed method and detailed explanation of applying the proposed method for the segmentation of the brain tumor from the magnetic resonance images. Experimental results illustrating the advantages of our method over the different methods are discussed in section 4 followed by the conclusion in section 5.

II. Background

In this section, we will discuss about the brain tumor and their types present in the brain. Some of the related works based on the segmentation are discussed in detail.

A. Brain Tumor

A brain Tumor is an intracranial mass produced by an uncontrolled and unwanted growth of cells found in the brain such as neurons, lymphatic tissue, skull, any other places or spread from other organs where cancer has taken place. Brain tumors are classified based on the type of tissue involved, the location of tumor, whether it is benign or malignant, and other considerations.

Primary brain tumors are the tumors that originated in the brain and are named for the cell types from which they originated. They can be benign (non-cancerous), meaning that they do not spread elsewhere or invade surrounding tissues. They can also be malignant and invasive.

Secondary brain tumors take their origin from tumor cells which spread to the brain from another location in the body. Most often cancers that spread to the brain to cause secondary brain tumors originate in the breast, kidney or from melanomas in the skin.

B. Classification of Brain Tumor

The classification of primary brain tumors is usually based on the tissue of origin, and occasionally on tumor location. The degree of tumor malignancy is determined by the tumor's histo-pathological features.

1. Classification of Brain Tumor by WHO

Here we study the properties and characteristics of most common tumors of WHO classification.

Gliomas

A brain tumor that develops from glial cells is called glioma. About half of all primary brai tumors and one-fifth of all primary spinal cord tumors form from glial cells.

Astrocytoma

Astrocytomas are primary brain tumors derived from connective tissue cells called astrocytes, which are star-shaped glial cell. They are most common type of the brain tumors and account about 40% of all primary brain tumors.

Ganglioglioma

These are slowly growing tumors occurring in children and young adults. Temporal lobes and cerebellar hemisphere are the most common locations for this type of tumors.

Oligodendroglioma

Oligodendrogliomas are the most common type of glioma, traditionally thought to comprise 2% to 5% of primary brain tumors and 4% to 15% of gliomas. It is believed that, in past, many tumors that were actually oligodendrogliomas were diagnosed to be various types of astrocytomas.

Ependymoma

These are glial tumors that arise from ependymal cells within the brain. This tumor is histologically benign but behaves malignantly. Intracranial lesions usually arise from the roof of the fourth ventricle in children, while spinal ependymomas typically occur in adults.

Medulloblastoma

In the brain, medulloblastoma most often arises in the posterior fossa. The tumor has potential of spreading throughout the CNS.

Lymphoma

Lymphomas typically develop in the sub-cortical and subependymal white matter. Within the brain substance, the irregular tumor edge extends along perivascular spaces. Lymphoma tumors are often multiple with central necrosis in AIDS.

Meningioma

Meningiomas are the most common benign tumors, accounting for 25%-30% of all primary brain tumors. They are most commonly located in the para-sagittal region. They are more common in women (3: 1) and occur in middle-aged and elderly patients.

Craniopharyngioma

Craniopharyngiomas develop in the area of the brain called the hypothalamus, which is close to the pituitary gland. It is usually found in children or young adults and accounts for around 1% of all brain tumors.

Pituitary adenoma

Pituitary adenomas comprise about 7% of primary brain tumors, they arise from the anterior lobe of the pituitary gland.

2. Classification of Brain Tumors Based on their Location

We can classify the brain tumors based on their location in to 3 classes

Local tumors: Local tumors confined to one hemisphere in one part of the brain.

Regional Tumors: it cross midline or tentorium invades bone, blood vessel, nerves and spinal cord.

Distant tumors: they are extended to nasal cavity, nasopharynx , posterior pharynx and outside the CNS.

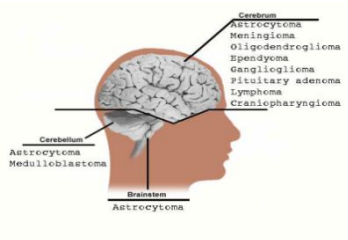

Fig. 2.1 Various types of brain tumors in various places in the central nervous systems

3. Classification of Brain Tumor Based on their Radiologic Appearance

Based on radiological appearance of tumors in contrast enhances T1-weighted and without considering the histology of tumors, we can classify the brain tumors into 4 classes: non-enhanced, fully-enhanced without edema, full-enhanced with edema and ring-enhanced tumors.

Non-enhanced tumors

Tumors of this type do not take contrast agent and appear hypo-intense in contrast enhances T1-weighted images. They are usually without edema or little edema.

Full-enhances tumors without edema

These tumors are without edema and appear hypo-intense in T1-weighted images and hyper-intense in T2-weighted and FLAIR images.

Full-enhanced tumors with edema:

These tumors have two sections, the solid section which appears in contrast enhanced T1-weighted images and hypo-intense in T1-weighted images and edema appears hypo-intense in T1-weighted images and contrast enhanced T1-weighted images.

Ring Enhanced Tumors:

These have 3 sections, central section is necrosis, solid section surrounds the necrosis and edema which surrounds the solid section.

4. Classification of Brain Tumor Based on their Alterations

We classify the brain tumors according to their spatial characteristics and the nature of the potential alterations of the brain structural organization.

Small deforming tumors (SD)

These are the tumors that are principally infiltrating or non-enhanced without necrosis or small necrotic tumors. The whole structural brain arrangement is not significantly altered.

Large deforming tumors (LD)

These tumors are necrotic and can be surrounded by a lot of edema. These tumors usually take contrast agent and are malignant.

C. Overview of Related Works

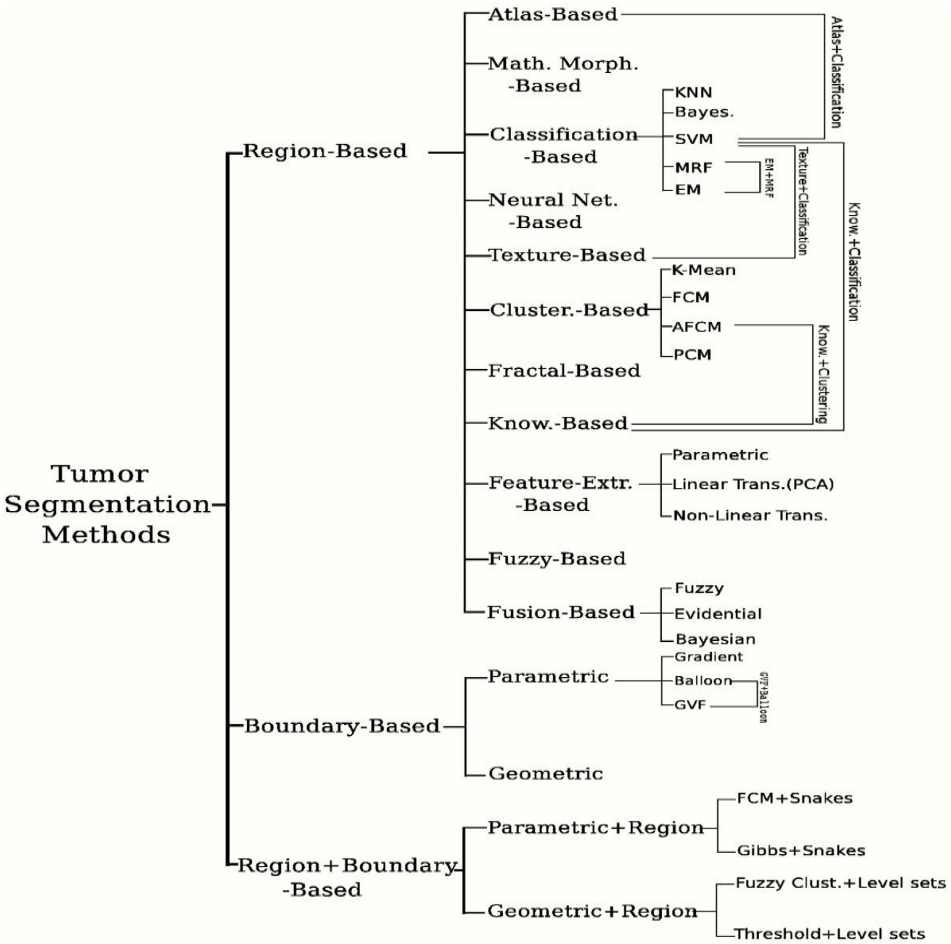

Fig. 2.2 Classification of different segmentation method

Several approaches has been proposed in the field of tumor segmentation. Lee et.al. [1] evaluated the use of support vector machine (SVM) classification method and MRFs for brain tumor segmentation and claimed the superiority of SVM-based approach. Fuzzy-correctedness is a useful method that has been adapted for measuring the tumor volume in MR images [2,3]. Markov random fields (MRFs) are also popular models for many medical image processing

mostly used in segmentation [4,5]. Recently, Corso et.al [6] applied the extended graph-shifts algorithm for image segementation.

One of the most powerful method that has been applied for the image segmentation is Active Contour. The basic idea is to evolve a curve around the object to be detected, and the curve moves towards its interior normal and stops on the true boundary of the object based on minimization energy. We can classify the active contours method as snake [7] and level set methods proposed by Osher and Sethian [8]. Snake is a semi-automatic method based on an energy minimizing spline guided by external constraint forces and pulled by image forces toward the contours of targets. The main drawbacks of snake method are its sensitivity to initial conditions and the difficulties associated with topological changes for the merging and splitting of the evolving curve. In recent years, the level set method has become a popular due to its ability to handle the complex geometries and topological changes. In comparison with the snake model, level set methods depends on full-domain energy minimization to implicitly represent the evolution curves and utilize the concepts of dynamics to guide the evolving curve. The level set is in fact a shape driven tool which using a properly defines speed function , can grow or shrink to take the shape of any complex of object of interest. Unlike the traditional deformable model, the level set method does not depend on the parameterizations of the surface [9]. This makes it very attractive and flexible in shape modeling and image segmentation. Another attractive advantage of level set method is that, given an initial zero level set, the entire segmentation procedure is fully automatic. In level set method, initial contour can be anywhere with arbitary size and the position of initial contour does not effect the final result. However, there are difficulties in using level sets that makes them less useful in some circumstances. One problem is that the level set formulation entail the tuning of several parameters. In some methods like [10-12], the interactive rates for solving the level set partial differential equation give the user immediate feedback on the parameters

and control the shape of the level set in real time. But the main short comings of such method is that they increase user interaction and gives better segmentation result if the user is familiar with the level set method and the region of interest. Leventon et al. [13], provides an automatic and more generic method for segmentation of tumor through the combination of level set evolution with statistical shape constraints. The main drawback of this method is that it may be difficult to obtain statistical prior knowledge in many cases, especially for tumor segmentation.

The existing level set method can be categorized into two classes: edge-based methods and region based methods. Edge-based methods stop the evolving contours by applying image gradient. These models are composed of an edge-based stopping term and a force term to control the motion the contour. But the calculation of the force term is a difficult task. Edge based models use local edge information to attract the active contour toward the object boundaries. Since it uses the edge information and do not assume homogeneity of image intensities thus can be applied for the images with intensity inhomogeneities. However, this method is sensitive to initial conditions and often suffers from serious boundary leakage problems in images with weak object boundaries.

One of the most popular edge-based models is the GAC model [14, 15], which utilizes image gradient to construct an edge stopping function (ESF) to stop the contour at the object boundary. Usually, a positive, decreasing and regular ESF $g(|\nabla I|)$ is used such that $\lim_{t\to\infty} g(t) = 0$. For instance,

$$g(|\nabla I|) = \frac{1}{1+|\nabla G_\sigma * I|^2}\ , \qquad \textbf{(2.1)}$$

Where $G_\sigma * I$ denotes convolving image with Gaussian kernel whose standard

deviation is σ. For digital images the discrete gradients are bounded and then ESF in Eq. (2.1) will never be zero in edges. In some active contour model the balloon forces are introduce to shrink or expand the contour which is very difficult to design. The large balloon force causes the contour to pass through the weak edges of the object. However, if the balloon force is not large enough, then the contour may not pass through the narrow part of the object. The drawback of the edge based model is failing to detect the boundaries when the initial contour is far from the desired object boundary. However, when compared with the edge-based models with region-based models, region-based models have several advantages. Region based models automatically offers a closed contour while edge based models should have an extra step to obtain complete region contours. Region-based models aim to identify each region of interest by using a certain region descriptor to guide the motion of the active contour. Region based models utilize the statistical information inside and outside the contour to control the evolution of curve and is independent of edge information therefore it has better performance over the images which has weak edge boundaries and it is also less sensitive to the initial position of the contours. The popular region-based method active contour models [16-19] depend on intensity homogeneity in each of the regions to be segmented. In fact, intensity inhomogeneity occurs in real images from different modalities. In medical images, intensity inhomogeneity occurs due to technical limitations or artifacts introduced by object being imaged. However, intensity inhomogeneity in magnetic resonance images arises from the non-uniform magnetic fields produced by radio-frequency coils as well as from variations in object susceptibility. Segmentation of such MR images usually requires intensity inhomogeneity correction.

One of the most popular region-based models is the C-V model [16], which is based on Mumford-Shah segmentation techniques [20] and has been successfully applied for the image segmentation. The C-V method has the ability to detect all of the contours irrespective of where the initial contours begin in

the image. Therefore, CV method is used to segment all the objects in the image using global segmentation. When compared with the GAC method, GAC can only segment the objects where the initial contour surrounds the boundary of the object.

1. The GAC and C-V Models

Geodesic active contour and Chan Vase methods are very useful algorithm used for the segmentation of objects. These are widely used in the medical field for the segmentation of the defected parts and orgrans in the medical imaging.

a. The GAC Model

Let Ω be a bounded open subset of R^2 and I:[0,a]×[0,b]→ R^+ be a given image. Let C(q):[0,1]→R^2 be a parameterized planar curve in Ω. The GAC model is derived by minimizing the following energy functional:

$$E^{GAC}(c) = \int_0^1 \underbrace{g(|\nabla I(C(q))|)}_{attraction\,term} \underbrace{|\frac{\partial C}{\partial q}(q)|dq}_{Regularity\,term} \qquad (2.2)$$

Where, g is the ESF as in Eq. (2.1).

The minimization of the objective function is done using a gradient descent method. Therefore, the initial curve $C_0(.)$ is deformed towards a (local/global) minimum E^{GAC}(c) according to the following equation

$$C_t = g(|\nabla I|)kZ - (\nabla g(\nabla I).Z)Z \qquad (2.3)$$

Normally, a constant velocity term α is added to increase the propagation

speed. Then, Eq. (2.3) can be written as

$$C_t = g(|\nabla I|)(k+\alpha)Z - (\nabla g(\nabla I).Z)Z \ , \qquad (2.4)$$

Where, g is the ESF as in Eq. (2.1), denotes the time as the contour evolves, Z is the inward normal to the curve, and k is the curvature of the contour.

From the above equation we can see that, two forces are acting on the contour, both in the direction of the inward normal:

· $g(|\nabla I|)(k+a)Z$ moves the curve towards the real object boundaries constrained by the curvature effect which ensures regularity during propagation.

· $\nabla g(|\nabla I|).Z)Z$ is applicable only around the real object boundaries $[\nabla g(|\nabla I|) \neq 0]$ and has a two roles to play. The first one is to attract the curve to the real boundaries and to overcome along them the propagation constraints imposed by the curvature effect and next is it is used as a refinement term that centralizes the curve to the real object boundaries.

The level set formulation for the corresponding equation is as follows:

$$\frac{\partial \varnothing}{\partial t} = g|\nabla \varnothing|\left(div\left(\frac{\nabla \varnothing}{|\nabla \varnothing|}\right)+\alpha\right)+ \nabla g.\nabla \varnothing \qquad (2.5)$$

Where, α is the balloon force which controls the contour expanding or shrinking inside or outside the object boundaries.

b. C-V Model

Chan and Vese [16] proposed an Active contour method as a special case of Munford-Shah problem [20]. For a given in domain, Chan and Vese model can be written by minimizing the following energy functional:

$$E^{CV} = \lambda_1 \int_{inside(C)} |I(x) - C_1|^2 dx + \lambda_2 \int_{outside(C)} |I(x) - C_2|^2 dx, \quad x\epsilon\, \Omega \qquad (2.6)$$

Where $inside(C)$ and $outside(C)$ represent the regions inside and outside the contour C, respectively, C_1 and C_2 are two constants which are the average intensities in $inside(C)$ and $outside(C)$ respectively. However, C_1 and C_2 can be away from the original image, and if the intensities within $inside(C)$ or $outside(C)$ are inhomogeneous, they do not contain any local intensity information, which is very crucial for the image segmentation with intensity inhomogeneity. Within the level set method, the following assumption is made:

$$\begin{cases} \{x \in \Omega : \varnothing(x) > 0 = inside(C)\}, \\ \{x \in \Omega : \varnothing(x) = 0\} = C, \\ \{x \in \Omega : \varnothing(x) < 0 = outside(C)\}, \end{cases}$$

Now, the value of C_1 and C_2 can be determined by minimizing Eq.(2.6) as given below.

$$C_1(\varnothing) = \frac{\int_\Omega I(x).H(\varnothing)dx}{\int_\Omega H(\varnothing)dx}, \tag{2.7}$$

$$C_2(\varnothing) = \frac{\int_\Omega I(x).(1-H(\varnothing))dx}{\int_\Omega (1-H(\varnothing))dx}, \tag{2.8}$$

We obtain the variational level set equation by incorporating the length and area energy terms into Eq. (2.6) as follows:

$$\frac{\partial \varnothing}{\partial t} = \delta(\varnothing)\left[\mu \nabla\left(\frac{\nabla \varnothing}{|\nabla \varnothing|}\right) - q - \lambda_1 (I - C_1)^2 + \lambda_2 (I - C_2)^2\right], \tag{2.9}$$

Where, $\mu \geq 0, q \geq 0, \lambda_1 \geq 0, \lambda_2 \geq 0$ are fixed parameters, μ controls smoothness of zero level set, q increases the propagation speed, and λ_1 and λ_2 control the

force inside and outside the contour, respectively. ∇ is the gradient operator. $H(\varnothing)$ is the Heaviside function and $\delta(\varnothing)$ is the Dirac function.

In numerical implementation, the Heaviside function $H(\varnothing)$ is replaced by a smooth function that approximates $H(\varnothing)$, called the smoothed Heaviside function H_ϵ, which is defined by

$$H_\epsilon(x) = \frac{1}{2}\left[1 + \frac{2}{\pi} arctan\left(\frac{x}{\epsilon}\right)\right], \tag{2.10}$$

Accordingly, the Dirac delta function $\delta(\varnothing)$, which is the derivative of the Heaviside function $H(\varnothing)$, is replaced by the derivative of H_ϵ, and is computed by

$$\delta_\epsilon(x) = H_\epsilon^{'}(x) = \frac{1}{\pi} \cdot \frac{\epsilon}{\epsilon^2 + x^2}, \tag{2.11}$$

III. The Proposed Method

In this section, we describe a system to extract the brain tumor from magnetic resonance images. The proposed algorithm attempts to extract the tumor irrespective of its shape and size.

A. Level Set Model and SPF

In order to precisely segment the brain tumor, the region based level set method with the modified SPF function is used. The SPF function defined in [26] has range of value between [-1, 1]. It changes the signs of the pressure of forces inside or outside the interested object. The contour shrinks if it is outside the interested object and expands if it is inside the object to locate the exact objected that has to be determined. Similarly, the spf function defined in [25] is

$$spf(I(x)) = \frac{I(x) - \frac{C_1 + C_2}{2}}{\min\left(|I(x) - \frac{C_1 + C_2}{2}|\right)}, \quad x \in \Omega \tag{3.1}$$

The modified SPF for the detection of brain tumor for segmentation is as follows:

$$spf(I(x)) = \frac{I(x) - \frac{C_1 + C_2}{2} - \alpha(i) + \rho(i) \times (\log \times \nabla)^2}{\min\left(|I(x) - \frac{C_1 + C_2}{2}|\right)}, \quad x \in \Omega \tag{3.1}$$

Where C_1 and C_2 are calculated from Eq. (2.7) and Eq. (2.8) respectively. In the modified SPF function, $\alpha(i)$ and $\rho(i)$ are the parameters that helps the contour to move smoothly inside and outside the interested object which is

calculated later. ∇ is the gradient operator. The addition of these terms are very useful for the movement of contour smoothly towards the targeted object. $I(x)$ is the given image and Ω is a bounded open sub-set of R^2.

Here, we suppose that the intensities inside and outside the object are nearly same regarded as C_1 and C_2 respectively.

The assumption of $C_1 < C_2$ is made. It is intuitive that $Min(I(x)) \leq C_1$, $Max(I(x)) \geq C_2$, therefore

$$Min(I(x) < \frac{C_1 + C_2}{2} < Max(I(x)),\ x \in \Omega \qquad (3.2)$$

It is obvious that, the signs of the spf in Eq. (3.1) are identical to the contour location. It also produces the pressure force to the different directions to push the contour towards the object.

Substituting the spf function in Eq. (3.1) for the ESF in Eq. (2.5), the level set formulation of the proposed model is as follows:

$$\frac{\partial \varnothing}{\partial t} = spf(I(x)).|\nabla \varnothing| \left(div\left(\frac{\nabla \varnothing}{|\nabla \varnothing|} \right) + \alpha \right) + \nabla spf(I(x)).\nabla \varnothing),\ x \in \Omega \qquad (3.3)$$

B. Implementation

In traditional level set methods [14, 27-29], the level set function $\varnothing$ may develop shocks, very sharp or flat shape during the evolution, which causes the further computation highly inaccurate. In order to avoid these problems, we can initialize the function $\varnothing$ as a signed distance function before the evolution and then re-initialize the function $\varnothing$ to be a signed distance function periodically during the evolution. Unfortunately, the side effect of moving the zero level set away from its interface exists in many of re-initialization methods. From the practical viewpoints, the re-initialization process is quite complicated and expensive. Therefore, the Gaussian filter is used to regularize the level set

function after each iteration.

We know that in the traditional method, the curvature based term, $\left(div\frac{\nabla \varnothing}{|\nabla \varnothing|}\right)|\nabla \varnothing|$ most of the time is used as a regularization term to regularize the level set function $\varnothing$. We know that in sine distance function, $|\nabla \varnothing = 1|$ which is true for all points except if they are equidistance from at least two points on the interface which is called skeleton but the existence of the skeleton does not cause any issues with the numeric as it will be smoothed with the time and does not affect the numerical solution to the level set equation. Since $\varnothing$ is an SDF function which satisfies $|\nabla \varnothing = 1|$, the regularized term can be written as $\triangle \varnothing$, which is the Laplacian of the level set function $\varnothing$. As mentioned in [30] and based on the theory of scale-space [31], the evolved function of the Laplacian is equivalent with Gaussian Kernel filtering the initial condition of the function. Therefore, regularization of the level set function is performed by the Gaussian filtering. The standard deviation value of the Gaussian filter controls the regularization strength. This standard deviation value is calculated automatically for the different kinds of images which reduce the workload of setting the value manually for the different images. As we have used Gaussian filter to smooth the level set function to keep the interface regular, the regular term $\left(div\frac{\nabla \varnothing}{|\nabla \varnothing|}\right)|\nabla \varnothing|$ is unnecessary in Eq. (3.3) and in addition our method utilizes the statistical information of region, the term $\nabla.\nabla \varnothing$ is unnecessary in Eq. (3.3). Therefore level set method can be written as

$$\frac{\partial \varnothing}{\partial t} = spf(I(x)).\alpha|\nabla \varnothing| + spf(I(x))\ x \in \Omega, \tag{3.4}$$

In the final level set equation, we add some terms which make more regularize and smooth to the level set method. In addition of those terms, the final level set equation for the proposed method can be written as

$$\frac{\partial \varnothing}{\partial t} = spf(I(x)).\alpha |\nabla \varnothing| + spf(I(x)) + (\log \times \sqrt{\alpha(i)})^2 - \sqrt{spf(I(x))} \quad x \in \Omega, \tag{3.5}$$

Where, $\alpha(i)$ is the parameter calculated automatically for each image.

C. Threshold and Parameter Calculation

In this section, we will calculate the different parameter used in the spf function and level set function used for deriving the contour towards the targeted object. These parameters are calculated using the mean and standard deviation of the object. In our proposed method different parameters are calculated automatically for the different kinds of images therefore it reduces the overload of tuning the parameter manually for different images. Since the parameters are set automatically proposed method is suitable for the inhomogeneous region. The mean and standard deviation denoted by μ and σ respectively are calculated by

$$\mu = \sqrt{\min\left\{\frac{1}{x \times y}\sum_{x=0}^{x-1}\sum_{y=0}^{y-1} I(x,y)\right\}}, \tag{3.6}$$

$$\sigma = \frac{1}{x \times y}\sum_{x=0}^{x-1}\sum_{y=0}^{y-1}(I(x,y) - \mu), \tag{3.7}$$

Where μ and σ are the mean and standard deviation of the image I. In Equ. (3.6), we calculate the mean value of each column in the image I and choose the minimum mean value and calculate its square root which is given by μ.

Here, we calculate the morphological gradient which is given by .

$$Morph_{grad} = \left\{\underbrace{(f \oplus b)(x,y)}_{dilation} - \underbrace{(f \ominus b)(x,y)}_{erosion}\right\}, \tag{3.8}$$

Where first part is the dilation operation and second part is the erosion operation

The addition of the morphological gradient with the image I produces the enhanced image

$$I_1 = Morph_{grad} + I, \tag{3.9}$$

Where I_1 is the enhanced image.

Now, the maximum mean value of the enhanced image is calculated as

$$\mu_1 = \max\left\{\frac{1}{x \times y}\sum_{x=0}^{x-1}\sum_{y=0}^{y-1} I_1(x,y)\right\}, \tag{3.10}$$

Where μ_1 and I_1 are the mean and enhanced image respectively.

We calculate the threshold value which is given by equation as below

$$T = \log\left(\sqrt{\sigma + \mu_1 - \mu}\right), \tag{3.11}$$

Where, μ, σ and μ_1 are calculated in Equ. (3.6), Eq. (3.7) and Equ. (3.10) respectively and T is the threshold value.

In the proposed method, Laplacian of the level set method is replaced by the Gaussian kernel. The standard deviation is the main parameter in Gaussian filter that regularizes the contour. In the proposed method, we replaced the standard deviation with the different parameter that regularizes the contour towards the object. The calculation of this parameter is done automatically for the different images instead of manually setting the parameter for different images.

The parameter used in the Gaussian filter in the proposed method is calculated as follows

$$Sig(\sigma_i) = \sum T_i + \log(T_i + 1), \tag{3.12}$$

Where $Sig(\sigma_i)$ is the parameter used in the Gaussian filter, T is calculated in Eq. (3.11) and i is the number of iterations. $Sig(\sigma_i)$ helps to regularize the contour in proposed method instead of the standard deviation that is used in the Gaussian Kernel.

Since we have calculated the parameter value that is used in the Gaussian Filter, we are going to calculate ρ the parameter value used in Eq. (3.1).

While using the contour function, we get the two output values say C and h. C contains the (x,y) coordinates and contour levels for contour lines, and h to a contour group object. The value of is calculated using the value stored in h returned by the contour function.

$$\rho = \log(\sqrt{h}), \tag{3.13}$$

Where, h is the value returned from the function contour in MATLAB.

Now, the value of α which is used in Eq. (3.6) and (3.5) are calculated as follows:

$$\alpha_i = \frac{(\rho(T+\sigma))}{\left(\log(Sig(\sigma_i))^2 \times \rho\right)}, \tag{3.14}$$

Where, $\sigma, T, Sig(\sigma_i)$, and ρ are calculated in Eq. (3.5), (3.11), (3.12) and (3.13) respectively. α_i is the value calculated in the i_{th} iteration.

D. Extraction of Tumor from Multiple Objects

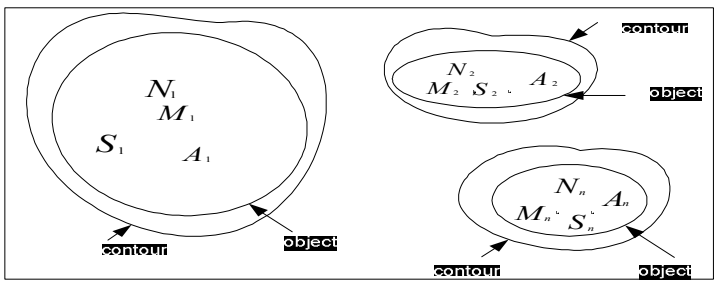

Fig. 3.1 **Demonstration of segmentation of Tumor from the multiple objects with different intensities.**

Since our method utilizes local image intensities and calculates the local standard deviation of the image, it somewhat can segment the multiple objects in the inhomogeneous condition also. The proposed method is focused on the extraction of tumor part from the brain MR images, therefore, we must remove the other objects that is not related to the tumor.

As shown in Fig. 3.4.1. We assume that there are $N_1, N_2, ..., N_n$ objects in the image, whose intensities are $M_1, M_2, ..., M_n$ respectively. The standard deviations of the objects are $S_1, S_2, ..., S_n$. The areas of the objects are denoted by $A_1, A_2, ..., A_n$. Since the contour are set around each object, it is very necessary to find the exact tumor object from the different objects presents in the image. For the thresholding process, the mean and standard deviation of each object having different areas are calculated. Therefore, the proposed algorithm applies the thesholding process to obtain the target object.

The following thresholding process is applied to extract the tumor part from the different objects.

$$idx(x,y) = N_n \geq M_n | N_n \geq S_n, \tag{3.15}$$

Where, N_n, M_n, and S_n are the objects, mean intensities and standard deviation of the object respectively. Each objects N_n that satisfied the Eq. (3.15) gives the output image $idx(x,y)$ which is the tumor image.

IV. Performance Evaluation

The dataset contains the MR images of 8 patients were acquired from the internet. The proposed method was tested with different MR images which have different shape, size and intensity. The given algorithm was tested using MATLAB 2010.

A. Subjective Quality

The subjective quality analysis is performed between proposed method, Chunming method, region growing method and Singh and Dubey method. Figure below shows the image obtained by proposed method and different methods. When the output images are viewed from the naked eyes, we can clearly see that the proposed method has better output result in comparison to the other methods. The proposed algorithm works well for all kinds of tumor images irrespective of its shape, size, location and its intensities. The evolution of the contour in different iteration in the proposed method is shown in the experimental results. Since, the proposed method can efficiently extract the tumor from brain in magnetic resonance images (MRI), our method outperformed the other method

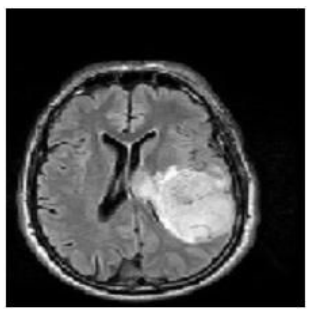

Fig.4.1 (a) Original image I

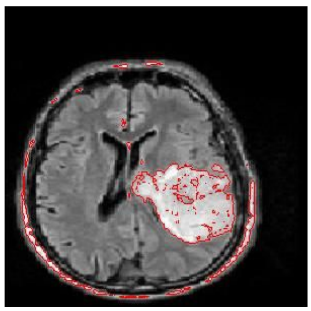

(a) 10th iteration

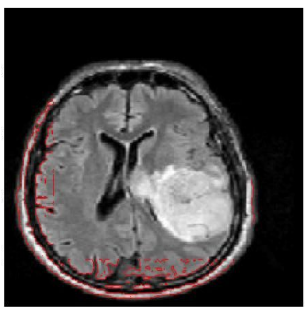

(b) 20th iteration

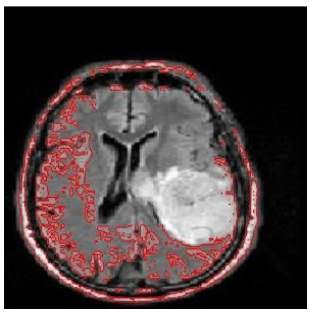

(c) 30th iteration

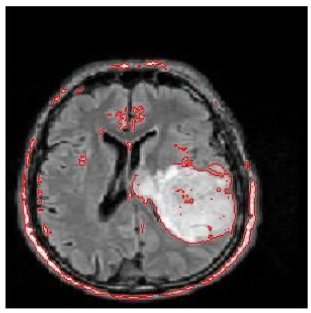

(d) 50th iteration

(e)120th iteration

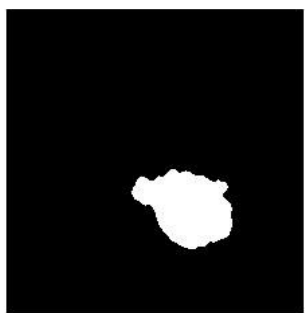

(f) Final Image

Fig 4.2 Segmented results using our proposed method.

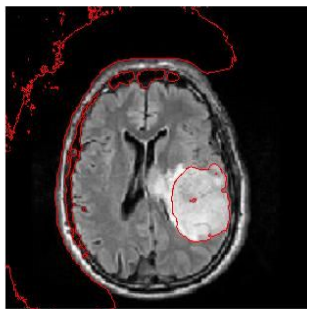

(a) 120th iteration

(b) Final Image

Fig 4.3 Segmented results using Chunming method

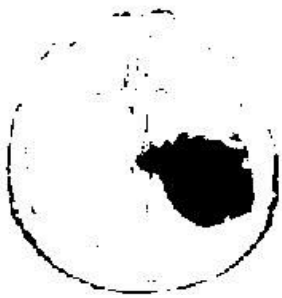

Fig. 4.4 (a) Segmented results using region grow method

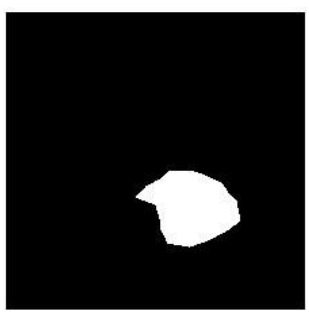

Fig. 4.5 (a) Segmented results using Singh and Dubey method

Fig. 4.2 shows the segmentation results of a brain tumor image with the objects having the week edges and with the different intensity. The size of the test image is 240×240. The fig. 4.1(a) is the original image. When the proposed method is applied to the original image, the contour begins and search for the targeted object. In Fig. 4.2(a) shows the beginning of the contour in the 10th iteration. In Fig. 4.2 we can see the evolving of the contour at different shapes. The contour is attracted slowly towards the object and it covers the different object. The evolving of the contour is till 120th iterations which is shown in fig. 4.2(e). At this iteration, the contour stops and surround the targeted object that is the tumor which occurs in the brain. (f) is the image obtained in the binary form from the proposed algorithm. During the experiment the value is calculated automatically which reduces the over head of setting the value manually.

Fig 4.3(a) and (b) are the image obtained from the Chunming Li method. From the figure, it is clear that, the Chunming method is unsuccessful to extract the tumor part of the brain. Chunming Li method after 120th iterations fails to surround the targeted object but the proposed algorithm after the 120th iterations have succeeded to surround the targeted object. The binary image obtained from the Chunming Li method contains a lot of noises and false tumor shape which is shown in Fig. 4.3(b) but if we compare the binary image obtained from the proposed method, it is clear that the our method has extracted the tumor successfully. Fig. 4.4(a) is the image obtained from the region growing technique. This technique also fails to extract the tumor part. We can clearly see that, the noises are also presents in the image. Singh and Dubey shown in fig. 4.5(a) is somewhat successful to extract the tumor part from the brain image but when compared with the proposed method Singh and Dubey method is unsuccessful to extract the all the tumor part but it has given the false shape of the tumor in the brain.

We test the more tumor MR images with the proposed method, Chunming Li method, Region Growing Technique and Singh Dubey method. The different results obtained from the different images are below

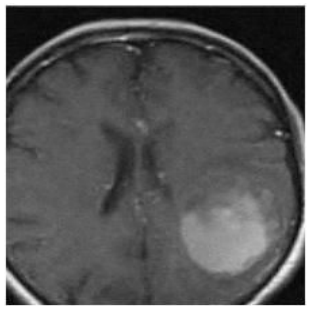

Fig.4.6 (a) Original image II

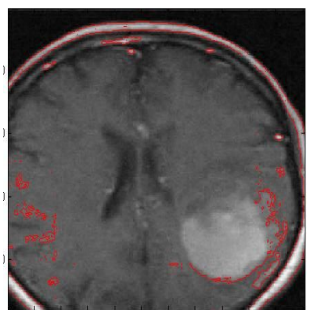

(a) 10th iteration

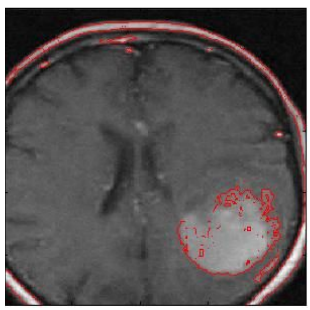

(b) 20th iteration

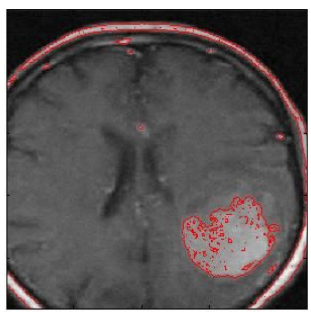

(c) 30th iteration

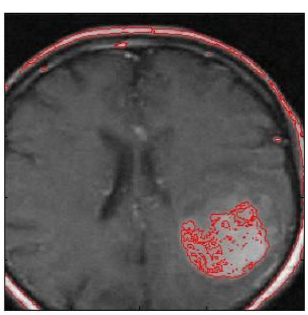

(d) 50th iteration

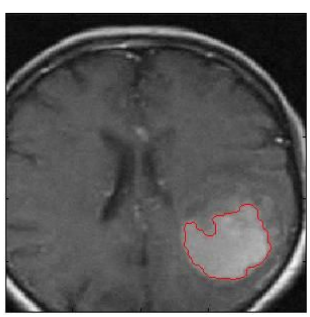

(e)120th iteration

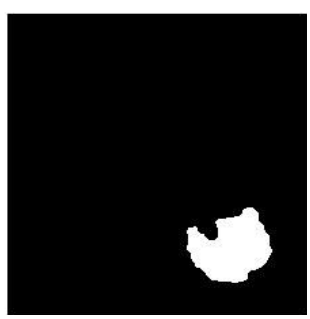

(f) Final Image

Fig 4.7 Extracted brain tumor using our proposed method

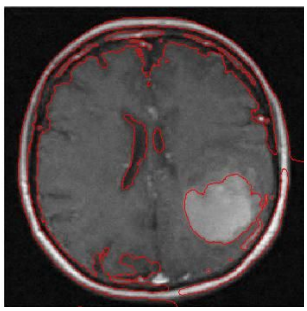

(a) 120th iteration

(b) Final Image

Fig 4.8 Extracted tumor using Chunming method

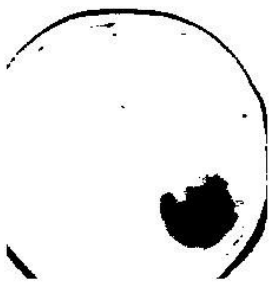

Fig. 4.9 (a) Extracted tumor using region grow method

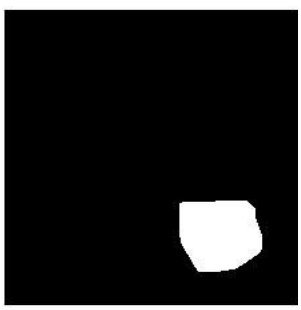

Fig. 4.10 (a) Extracted tumor using Singh and Dubey method

Fig. 4.6 – Fig.4.10 demonstrates the segmentation of the brain tumor using proposed method and other three different methods. Fig. 4.7 (a)-(f) are the images obtained using the proposed method. Fig. 4.6(a) is the original image. The different images obtained during the iterations are shown from (a) to (e) from proposed method. In Fig. 4.7(e) we can see that the contour surrounds the object which is the targeted object and (f) is the binary image obtained from proposed method. Fig. 4.8(a) is the image obtained after 120th iteration and (b) is the binary image obtained from Chunming Li method. In this method, the contour fails to surround the tumor part which is our desired object. The Chunming method has failed to segment the tumor part from the brain image. Fig. 4.9(a) is the output image obtained from the region growing technique. In this image, we can see that the image contain a lots of noises and Fig. 4.10(a) is the image obtained from the Singh and Dubey method which is based on the manual segmentation. Since we have to know the region of interest before segmenting the desired part, it is really a huge overload to the people. All the people should have knowledge about the tumor before segmenting the region of interest. People with the little knowledge about the tumor may misclassify the tumor part from the images. Therefore, this method is not suitable.

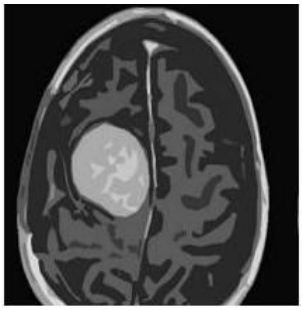

Fig.4.11 (a) Original image III

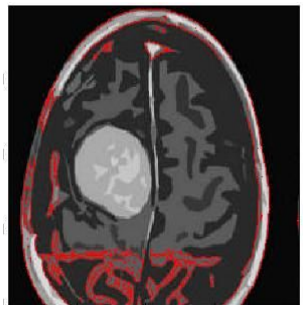

(a) 10th iteration

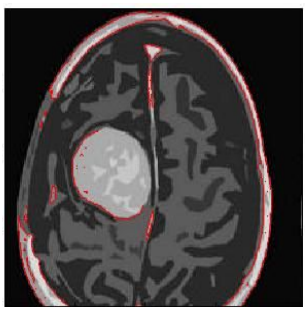

(b) 20th iteration

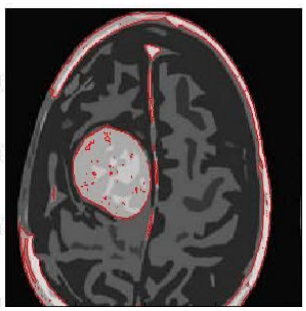

(c) 30th iteration

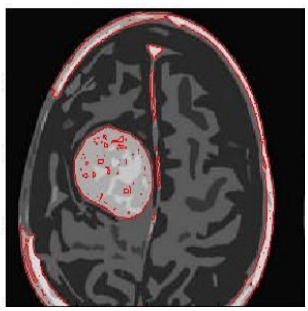

(d) 50th iteration

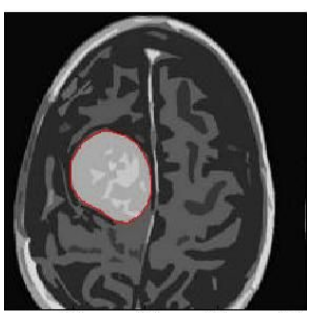

(e)120th iteration

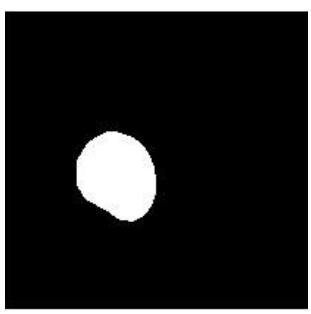

(f) Final Image

Fig 4.12 Segmented results of oval shape brain tumor using our proposed method

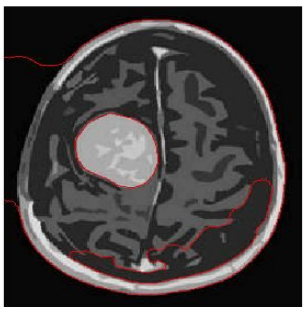

(a) 120th iteration

(b) Final Image

Fig 4.13 Segmented results of brain tumor having oval shaped using Chunming method

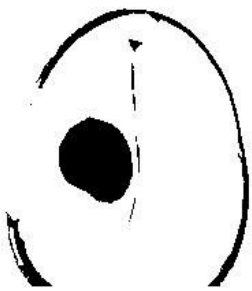

Fig. 4.14 (a) Segmented results of tumor having oval shaped using region grow method

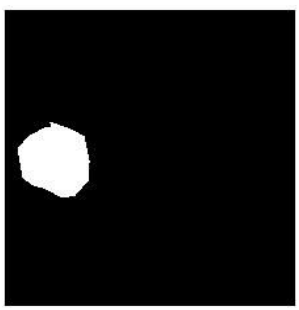

Fig. 4.15 (a) Segmented results of tumor having oval shaped using Singh and Dubey method

Fig. 4.11-4.15 shows the segmentation of brain tumor from magnetic resonance images. The size of the image is 200×200. Fig. 4.11(a) is the original image and Fig. 4.12(a)-(e) are the images obtained from proposed method in different iterations number and image (f) is the finally extracted image. Fig. 4.13(a) and (b) are the images obtained from the Chunming method. In Fig. 4.13 (a) Chunming Li method has been successful to extract the tumor part but it also has the false part of the brain. It fails to surround the tumor part of the brain only. In this case, the proposed method has outperformed the Chunming Li method. Fig. 4.14 (a) and Fig. 4.15 (a) are the images obtained from the region growing technique and Singh and Dubey method respectively. Proposed algorithm has better result than these two methods respectively.

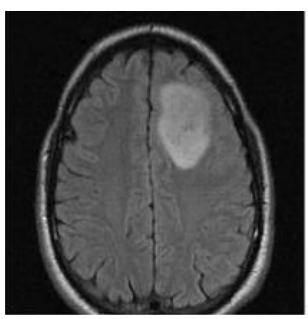

Fig.4.16 (a) Original image Ⅳ

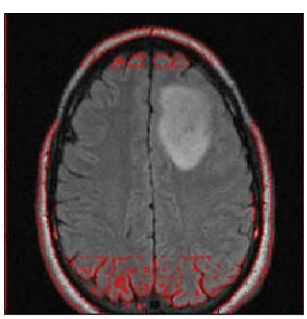

(a) 10th iteration

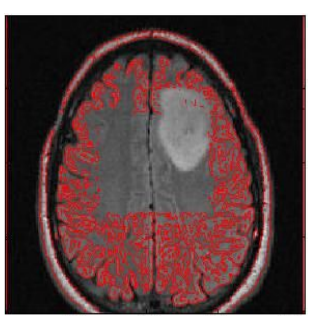

(b) 20th iteration

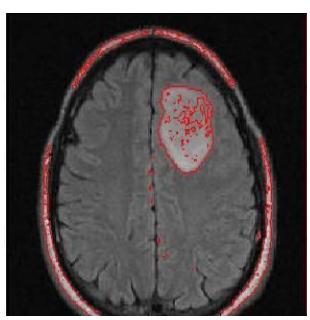

(c) 30th iteration

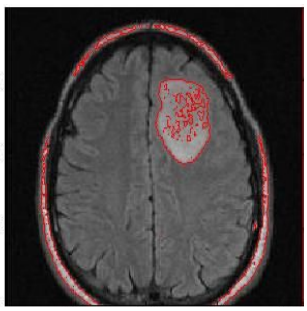
(d) 50th iteration

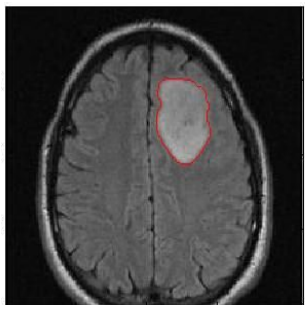
(e)120th iteration


(f) Final Image

Fig. 4.17 (a) Extracted brain tumor having low intensity using our proposed method.

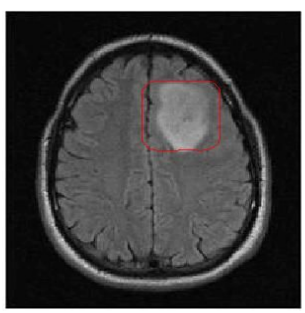
(a) 120th iteration

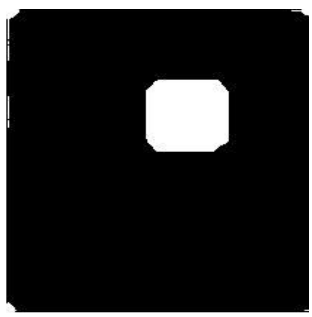
(b) Final Image

Fig. 4.18 Segmented results of brain tumor having low intensity using Chunming method

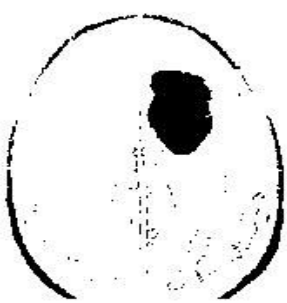

Fig. 4.19 Segmented results of brain tumor having low intensity using region growing method.

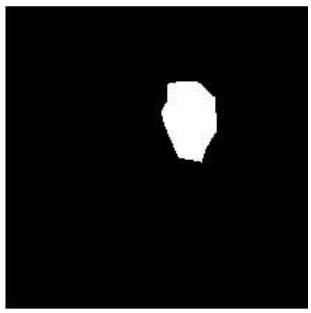

Fig. 4.20 Segmented results of brain tumor having low intensity using Singh and Dubey method.

Fig. 4.16 – 4.20 demonstrates the extraction of brain tumor from magnetic resonance images. The size of the image is 200×200. Fig. 4.16(a) is the original image and the images from Fig. 4.17(a) to (f) are the images obtained from the proposed method. Fig.4.18 (a) and (b) are the images obtained from the Chunming method. In proposed method the contour surround the exact part of the tumor where as in Chunming method the contour is in different shape which is different from the shape of the tumor. Fig. 19(a) and Fig. 20(a) are the images obtained from the region growing method and Singh and Dubey method respectively. Singh and Dubey method was successful to extract the tumor part but its shape differs from the tumor shape when compared with the real tumor part.

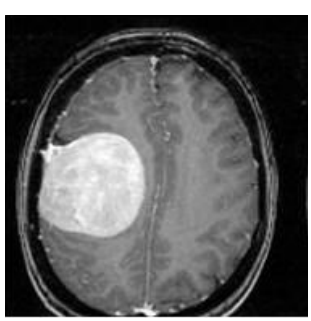

Fig. 4.21 (a) Original image V

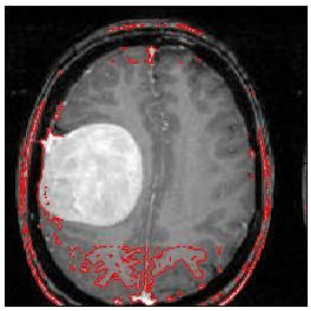

(a) 10th iteration

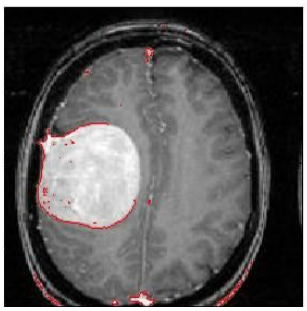

(b) 20th iteration

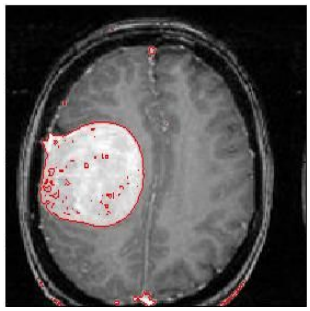

(c) 30th iteration

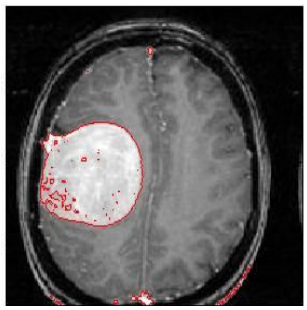

(d) 50th iteration

(e)120th iteration

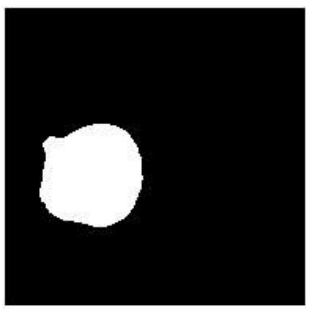

(f) Final Image

Fig. 4.22 (a) Extracted brain tumor having high intensity using our proposed method.

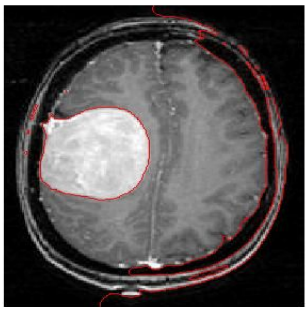

(a) 120th iteration

(b) Final Image

Fig. 4.23 Segmented results of brain tumor having high intensity using Chunming method

Fig. 4.24 (a) Segmented results of brain tumor having high intensity using region growing method

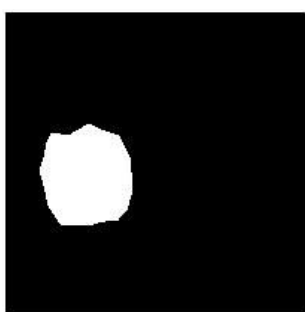

Fig. 4.25 (a) Segmented results high intensity tumor using Sing and Dubey method

Fig. 4.21-4.25 shows the extraction of brain tumor. Fig. 4.21(a) is the original image and Fig. 4.5(a)-(f) are the images obtained from the proposed method. The proposed method when compared with the other methods yields the better result. Chunming method gives the different shape from the shape of the tumor, region growing technique has unwanted parts which may cause difficult to identify the brain tumor and Singh and Dubey method somehow is able to extract the tumor part but the result of our method is better than their method.

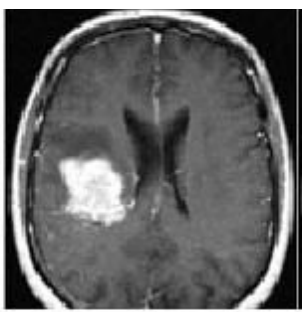

Fig. 4.26 (a) Original image VI

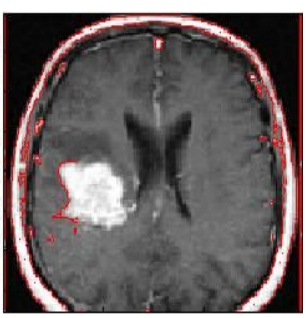

(a) 10th iteration

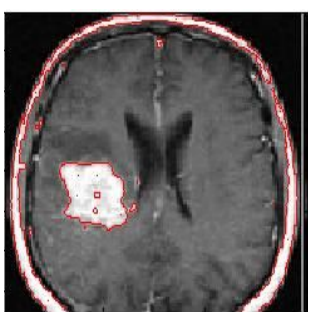

(b) 20th iteration

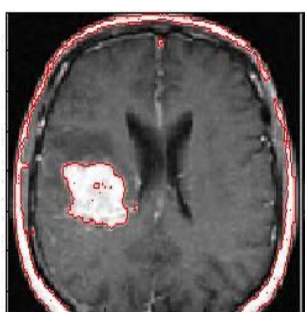

(c) 30th iteration

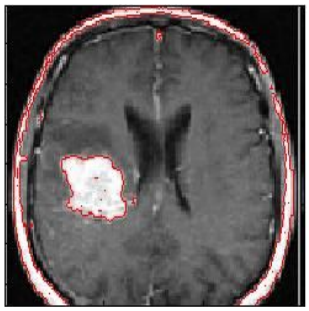

(e) 50th iteration

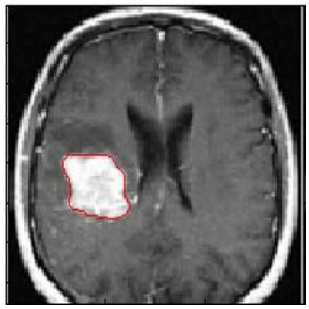

(f)120th iteration

(g) Final Image

Fig. 4.27 (a) Extracted star shaped tumor using our proposed method.

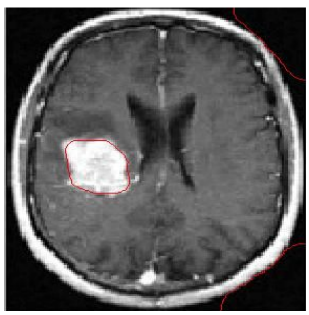

(a) 120th iteration

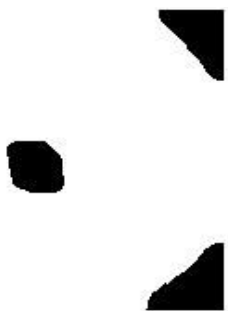

(b) Final Image

Fig. 4.28 Segmented results of star shaped tumor using Chunming method.

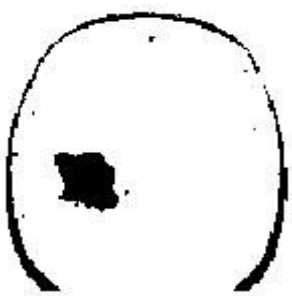

Fig. 4.29 (a) Extracted star shaped tumor using region grow method.

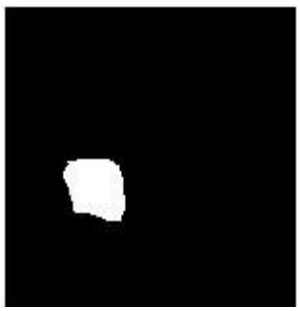

Fig. 4.30 (a) Segmented results of star shaped tumor using Singh and Dubey method.

Fig. 4.26-4.30 shows the output obtained from the proposed method, Chunming Li method, region growing technique and Sing and Dubey method. Fig. 4.26(a) is the original image, Fig. 4.27(a)-(f) are the images obtained from the proposed method. Fig 4.28(a) and (b) are the images obtained from the Chunming method and Fig. 4.29(a) and Fig. 4.30(b) are the images obtained from the region growing techniques and Singh and Dubey method respectively. Chunming method gives the false shape of the tumor. Region growing technique has a tumor part but it also contains other wanted parts. Singh and Dubey method has successfully extracted the tumor part but our method has outperformed the final result.

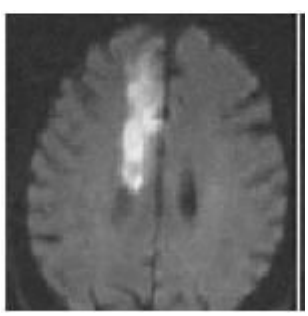

Fig. 4.31 (a) Original image VII

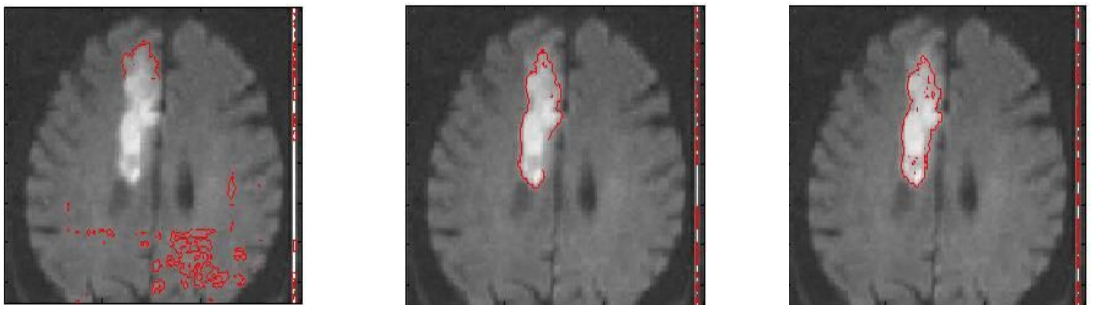

(b) 10th iteration (c) 20th iteration (d) 30th iteration

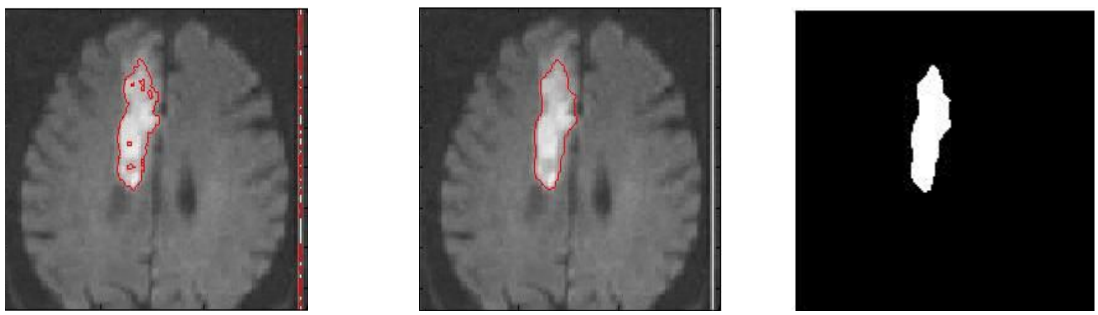

(e) 50th iteration (f)120th iteration (g) Final Image

Fig. 4.32 Brain tumor having cylindrical shape extracted from our proposed method

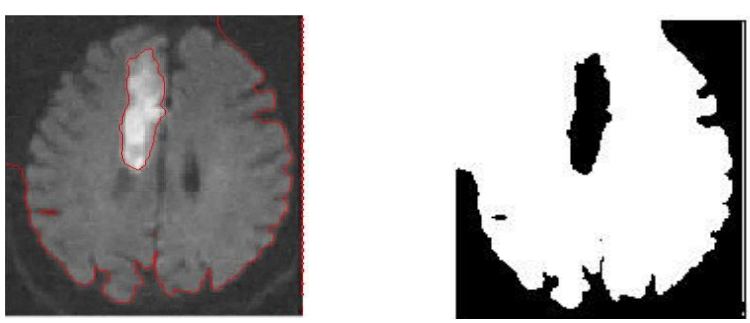

(a) 120th iteration (b) Final Image

Fig. 4.33 Extracted tumor having cylindrical shape using Chunming method.

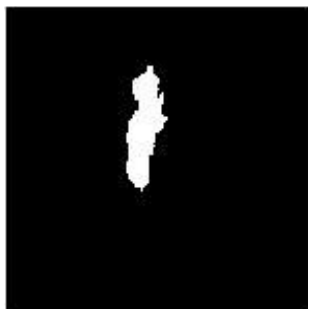

Fig. 4.34 Extracted tumor having cylindrical shape using region growing method

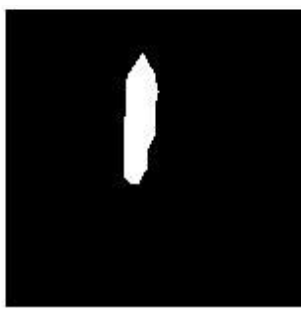

Fig. 4.35 Extracted tumor having cylindrical shape using Singh and Dubey method

Fig. 4.31 – Fig. 4.35 demonstrates the output result obtained from proposed method, Chunming Li method, region growing technique and Singh and Dubey method. Fig. 4.31(a) is the original image and Fig. 4.32(a)–(f) are the images obtained from the proposed method. Fig 4.33(a) and (b) are the images obtained from the Chunming method. Here, the contour surrounds the object but it also surrounds the false part of the brain in 120th iterations. But in the proposed method, in Fig. 4.32(e) after 120th iterations the contour is exactly around the object. Fig. 4.34(a) and Fig. 4.35(a) are the images obtained from the region growing technique and Singh and Dubey method respectively. Region growing technique and Singh and Dubey method has been successful to extract

the tumor part. The size of the image used in this experiment is 150×150.

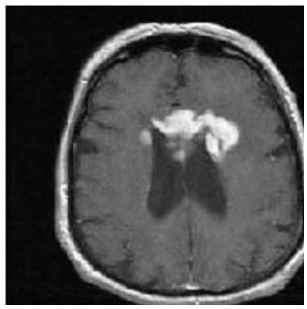

Fig. 4.36 (a) Original image VIII

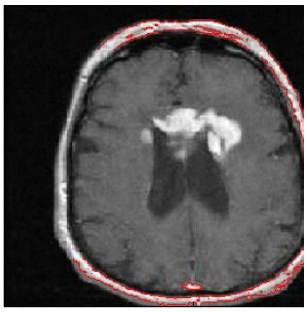

(b) 10th iteration

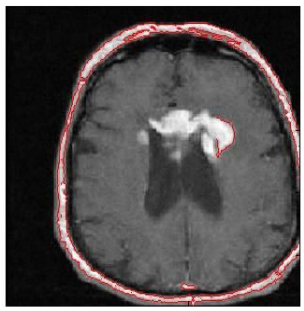

(c) 20th iteration

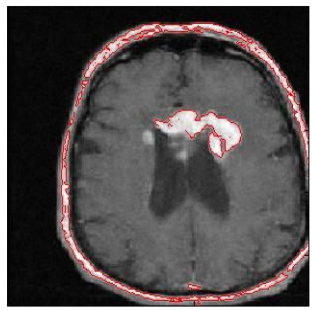

(d) 30th iteration

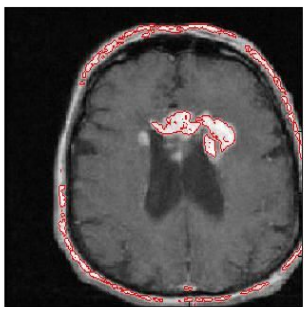

(e) 50th iteration

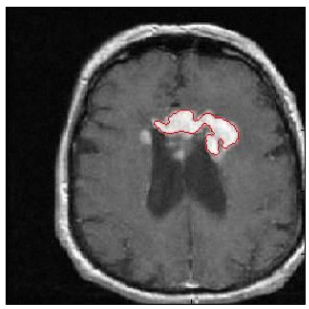

(f)120th iteration

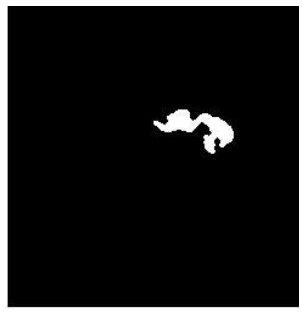

(g) Final Image

Fig. 4.37 Tumor having complex structure segmented using our proposed method

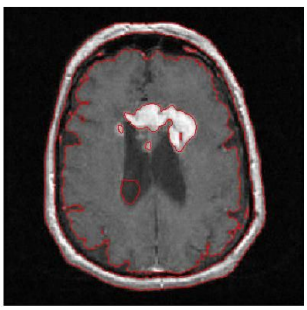

(a) 120th iteration

(b) Final Image

Fig. 4.38 Segmented results of complex tumor structure using Chunming method.

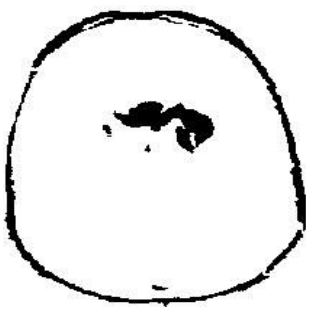

Fig. 4.39 Extracted complex tumor structure using region grow method.

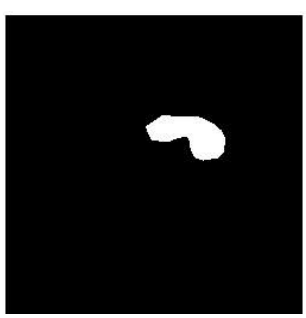

Fig. 4.40 Segmented results of complex tumor structure using Singh and Dubey method.

Fig. 4.37 shows our method in processing with the brain which consists of the tumor part. The size of the image is 200×200. Fig. 4.36(a) is the original image and Fig. 4.37(a)-(f) are the images obtained from the proposed method. In (a) we can see that the contour is not evolved to the targeted object in 10th iteration. But in (b) after 20th iterations the contour is near to the object and in 120th iterations shown in (e) in proposed method, the contour successfully surround the object. Fig. 4.38(a) and (b) are the images obtained from the Chunming Li method. Chunming method is successful to surround the object but we can see that it also contains some other unwanted parts. Fig 4.39(a) and Fig. 4.40(a) are the images obtained from the region growing technique and Sing and Dubey method respectively. When the output of both methods is compared with our method, the proposed method outperforms the final result.

Table 4.1 calculated value of different parameter.

Images	α	ρ	$Sig(\sigma_i)$
Fig. (4.2)	40.2	2.57	2.42
Fig. (4.7)	16.08	2.57	3.56
Fig. (4.12)	21.58	2.57	3.65
Fig. (4.17)	19.12	2.56	3.61
Fig. (4.22)	27.13	2.58	3.87
Fig. (4.27)	24.19	2.55	3.77
Fig. (4.32)	14.21	2.58	3.76
Fig. (4.37)	23.20	2.57	3.70

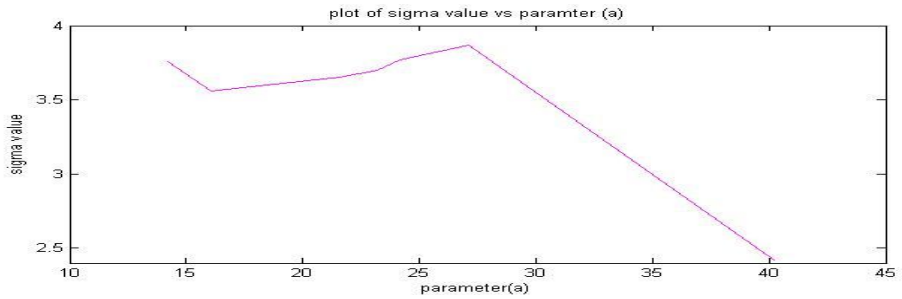

Fig. 4.41 plot of sigma value ($Sig(\sigma_i)$) and the value α.

Table 4.1 shows the value calculated for the different parameters that are used in the experiment. From the table we can see that the value of α and $Sig(\sigma_i)$ are different where the value of ρ are nearly same to the different images. The graph shows the value plot between α and $Sig(\sigma_i)$.

B. Segmentation Validation and Quantitative Analysis

The results of tumor segmentation over eight MR images for proposed method, Chunming method, region grow technique and Sing and Dubey method are compared with the manual segmentations. Fig. 4.1 to Fig. 4.40 shows the segmentation results by proposed method, Chunming, region grow and Singh and Dubey method on some of the test images. In this paper three validation techniques have been applied for the quantitative analysis of the different method. Let Q_m and Q_A denote the tumor voxels in the manual segmentation and the tumor voxels obtained from the different method. In this paper three validation techniques are used.

1. Jaccards' measure: Jaccards coefficient is widely used to calculate the spatial overlap measure for the pair of segmentations Q_m and Q_A. It can be expressed as a percentage as shown below

$$JM = \frac{|Q_m \cap Q_A|}{|Q_m \cup Q_A|} \times 100, \quad \textbf{(4.1)}$$

Where Q_m and Q_A are the tumor voxels segmented manually and the different methods.

The value obtained from the Jaccard's Measure from different methods is listed in table 4.2.

2 Dice Coefficient: it is one of a number of measures of the extent of spatial overlap between the two binary images. It is commonly used in reporting performance of segmentation and its value ranges from 0 which indicates no overlapping and 1 denotes perfect agreement. The dice values are expressed as percentage and obtained using Eq. (4.2.1)

$$DC = \frac{2 \times |Q_m \cap Q_A|}{|Q_m| + |Q_A|} \times 100, \quad \textbf{(4.2)}$$

Where Q_m and Q_A are the tumor voxels segmented manually and the different methods respectively.

The value of Dice Coefficients are listed in table 4.2 for different tumor images obtained from different methods.

3 Root mean square error (RMSE): it is a quadratic scoring rule which measures the average magnitude of the error. The $RMSE$ value is calculated as

$$RMSE = \sqrt{\frac{\sum_{i=1}^{n} (Q_m - Q_A)^2}{n}}, \quad \textbf{(4.3)}$$

Where Q_m and Q_A are the tumor voxels segmented manually and the different

methods respectively, $RMSE$ is the Root Mean Square Error value.

The value of JM, DC and $RMSE$ are listed in table below for different tumor images obtained from different methods.

Table 4.2 Competitive Results

Jaccards Measure (JM)				
Image index	Proposed method	Chumming Li	Region growing	Singh and Dubey
4.2-4.5	84.0	30.0	63.12	78.68
4.7-4.10	85.6	40.0	59.0	56.0
4.12-4.15	91.24	40.0	52.30	41.0
4.17-4.20	87.45	57.60	34.04	75.86
4.22-4.25	93.76	12.0	80.59	80.06
4.27-4.30	83.49	15.16	28.77	83.41
4.32-4.35	86.25	68.58	42.10	77.11
4.37-4.40	84.75	52.3	29.68	77.65

(a)

Dice Coefficient (D)				
Image index	Proposed method	Chumming Li	Region growing	Singh and Dubey
4.2-4.5	81.13	11.59	77.39	44.04
4.7-4.10	92.8	35.0	63.04	35.0
4.12-4.15	95.42	55.0	68.68	29.0
4.17-4.20	93.31	58.0	50.79	43.14
4.22-4.25	96.78	24.62	89.25	44.46
4.27-4.30	91.0	13.57	44.68	45.51
4.32-4.35	89.05	40.68	74	43.54
4.37-4.40	85.53	10.0	45.77	43.39

(b)

Root Mean Square Error (RMSE)				
Image index	Proposed method	Chumming Li	Region growing	Singh and Dubey
4.2-4.5	0.13	11.72	0.16	0.109
4.7-4.10	0.076	244.68	0.32	0.15
4.12-4.15	0.075	51.024	0.21	0.191
4.17-4.20	0.0716	336.08	0.25	0.1015
4.22-4.25	0.0748	135.0570	0.1687	0.074
4.27-4.30	0.078	196.03	0.276	0.074
4.32-4.35	0.087	0.11	0.20	0.087
4.37-4.40	0.083	29.68	0.22	0.081

(c)

Table 4.2 shows (a) Jaccards measure, (b) Dice coefficient, and (c) RMSE value

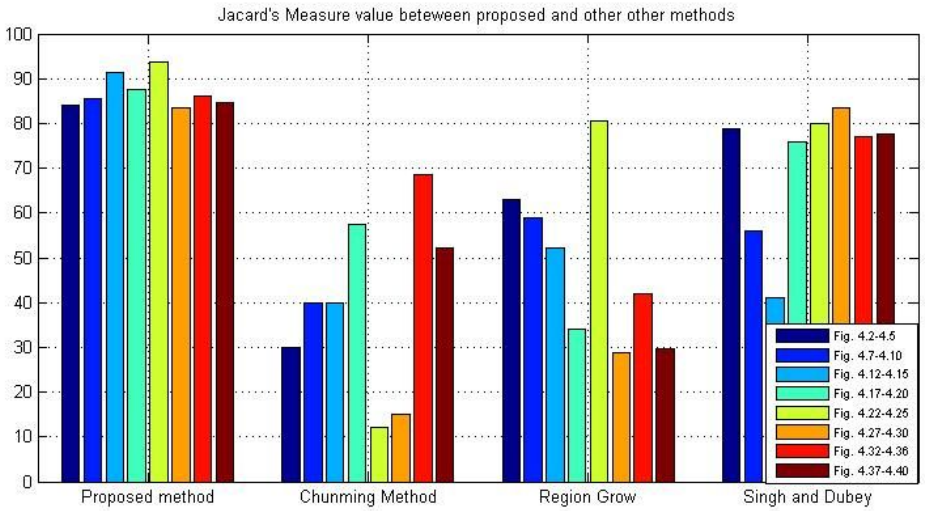

(a)

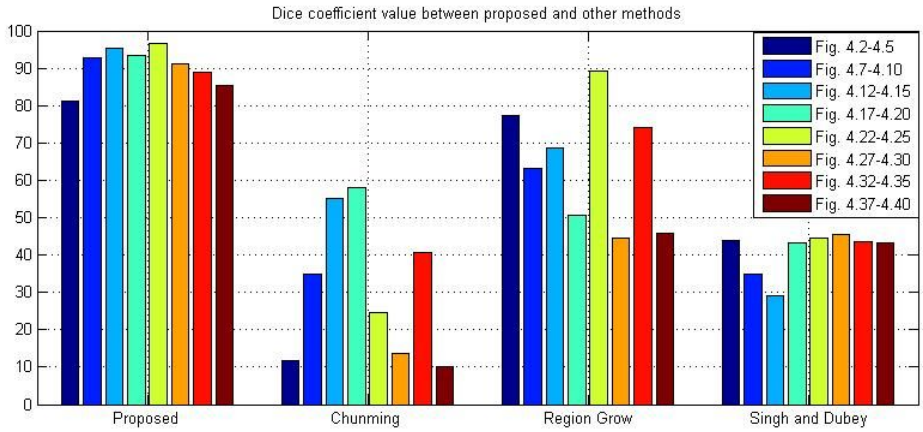

(b)

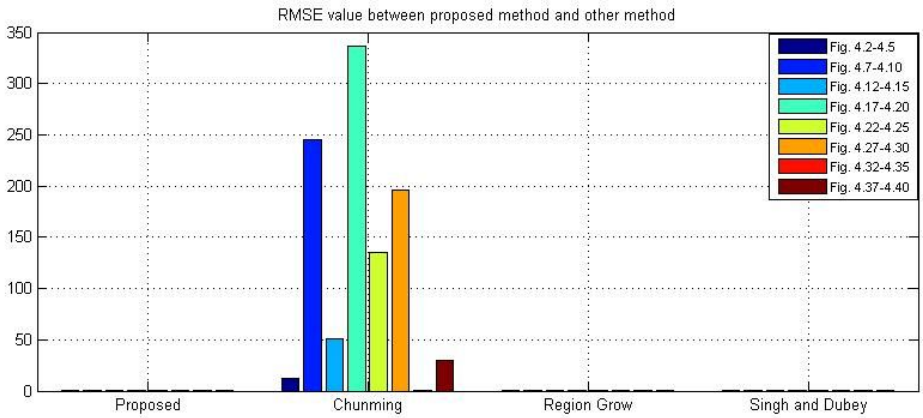

(c)

Fig. 4.42 Graphical Comparisons in terms of Jaccards measures, Dice Coefficient and Root mean square error obtained from table (a) 4.2.a, (b) 4.2.b, (c) 4.2.c.

The proposed method used Jaccards measure, Dice coefficient, and root mean square error value for the objective analysis between the proposed method, Chunming method, Region grow and Singh and Dubey method. Table 4.2(a) to (c) shows the value calculated for Jaccards measure, dice coefficient,

and root mean square error value for proposed, Chunming, region grow and Singh and Dubey method. Fig. 4.42 shows the graphical representation of those values. In fig. 4.42(a), we can see that the proposed method has got the JM value variation from 83.49% to 93.76%. Chunming, regions grow and Singh and Dubey method has the JM value variation from 12% to 68.58%, 28.77% to 80.59% and 41% to 83.41% respectively. The JM value for Fig. 4.32 and Fig.4.35 (a) obtained from proposed method and Singh and Dubey are nearly same, but for other images, values obtained from the proposed method is better than other method, the proposed method outperformed the other methods.

Fig. 4.42(b) compares the Dice coefficient for proposed, Chunming, regions grow, and Singh and Dubey method. As we can see in this figure, and also in Table 4.2(b), the variation of DC in proposed method, Chunming, region grow and Sing and Dubey method varies from 81.13% to 96.78%, 10% to 58%, 44.68% to 89.25%, 29% to 45.51% respectively. Thus, the result of proposed method is better when compared with other methods.

Fig. 4.42(c) shows the comparison of the root mean square error value for different images obtained from proposed and other methods. During the experiment we can see from fig. 4.42(c), the Chunming method has a large RMSE in comparison to proposed method and other two methods. Since the value obtained by proposed, region grow, Singh and Dubey method are very less, it is not seen clearly in the fig. 4.42(c). As we look at the Table 4.2(c), the RMSE is less for the proposed method in comparison to region grow and Singh and Dubey method. For Fig. 4.5, 4.30 and 4.40 RMSE value of Singh and Dubey method are less than the proposed method where as for Fig. 4.25 RMSE value is equal to proposed method. The RMSE value calculated from proposed method for other figures are less than the other methods.

When we compare the graph 4.42(a), (b), and (c) the proposed method outperformed the Chunming, region grow, Singh and Dubey method in three validation techniques. Therefore, proposed method is better than other three methods.

C. Complexity Analysis

In this section, we analyze the complexity of the proposed method with that of Chunming Lie Method based on the time complexity. The comparison with other two methods Region grow and Singh and Dubey is not performed because these two methods are not automatic and the output of these methods does not depend on the iteration. Table 4.3 below shows the calculation of time complexity performed on MATLAB 10, Intel 2.40 GHz, with memory 2.0 GB. From the table below, it is clear that, the time taken to run the proposed method is less than the Chunming method for every test image. Chunming method has more time complexity than proposed method because the contour has to be initialize on the object. The parameter has to be set manually. But in proposed method, these works are done automatically. Therefore, we can say that the proposed method has less time complexity in comparison with Chunming method and proposed method outperformed Chunming method.

Table 4.3 Total time taken to run the algorithm in seconds

Image index	Proposed method	Chunming Li
4.2-4.3	16.198	170.609
4.7-4.8	13.169	155.236
4.12-4.13	10.814	90.987
4.17-4.18	10.889	84.336
4.22-4.23	10.678	67.466
4.27-4.28	8.410	50.423
4.32-4.33	7.847	9.665
4.37-4.38	10.254	14.947

Ⅴ. Conclusion

Image segmentation plays a significant role in the extraction of different parts from the objects. In the modern era, the persons suffer from different diseases. The careful diagnosis is most necessary. The manual diagnosis may lead the death of the patients. Therefore, efficient extraction of the infected parts helps doctor to diagnosis the diseases in quick succession. This help to saves the time. In this case, our method is very helpful for the automatic extraction of the brain tumor from the MR images. Since, no manual calculation has to be performed, the proposed algorithm is helpful to the people with the low level knowledge about the tumor.

This thesis paper presents a class of algorithm for the extraction of brain tumor from MR images. The proposed algorithm segments the tumor from the brain images. Our method utilizes the region based method for the segmentation of the targeted object. The main advantages of proposed method are no matter where the contour evolves, the object is extracted efficiently. The contour evolves toward the object irrespective of its initialization and it grows and shrinks inside and outside the object to surround the targeted object part. There is no manual calculation, therefore it reduces the human error and there is no necessary of manually tuning the value of different parameters. The proposed method works well even if the image has inhomogeneous region. In the proposed method, we should not care of the edges of the image. The method is able to extract the tumor part efficiently even the image has weak edges.

Experimental results performed on different test images of brain tumor magnetic resonance images have excellent performance interms of both subjective and quantitative analysis in comparison of other method. Since, the final results of proposed method over the different magnetic resonance images are better than the other method, our method can be used efficiently for the extraction of the tumor from the brain.

References

[1] C. Lee, M. Schmidt, A. Murtha, A. Bistritz, J. Sander, and R. Greiner, "Segmenting Brain Tumor with Conditional Random Fields Model and Supprot Vector Machines," In proceeding of International conference on Computer Vision in Workshop on Computer Vision for Biomedical Image Applications, pp. 469-478, 2005.

[2] G. Moonis, J. Liu, J. Udupa, D. Hackney, "Estimating of Tumor Volume with Fuzzy-Connectedness Segmenation of MR images," AJNR Am J Neuroradiol, vol. 23, pp. 356-63, March 2002.

[3] J. Liu, J. Udupa,D. Odhner, D. Hackney, and G. Moonis, "A System of Brain Tumor Volume Estimation via MR imaging and Fuzzy Connectedness," Computerized Medical Imaging and Graphics, vol. 29, pp. 21-34, 2005.

[4] K. Held, E. Kops, B. Krause, W. Wells, R. Kikinis, H. Muller-Gartner, "Markov Random Field Segmentaiton of Braim MR images," IEEE Transactions on Medical Imaging, vol. 16, pp. 878-886, 1997.

[5] Y. Zhang, M. Brady, S. Smith, "Segmentation of Brain MR images Through a Hidden Markov Random Field Model and the Expectation Maximization Algorithm," IEEE Transactions on Medical Imaging, vol. 20, pp. 45-57, 2001.

[6] J. Corso, A. Yuille, N. Sicotte, A. Toga, "Detection and Segmentation of Pathological Strucutres by the Extended Graph-shifts Algorithm," In proceedings of Medical Image Computing and Computer Aided Intervention (MICCAI), vol. 1, pp. 985-994, 2007.

[7] M. Kass, A. Witkin, and D. Terzopoulos, "Snakes: Active Contour Models," Int. J. Comput. Vision, vol. 1, pp. 321-331, 1987.

[8] S. Osher and J. A. Sethian, "Fronts Propogating with Curvature-dependent Speed Algorithm based on Hamilton-Jacobi Formulations," J. Comput. Phys. vol. 79, pp. 12-49, 1988.

[9] J. A. Sethian, “Level Set Methods and Fast Marching Methods: Evolving Interfaces in Geometry, Fluid Mechanics, Computer Vision and Materials Science,” Second Ed. Cambridge University Press, 1999.

[10] M.Droske, B. Meyer, M. Rumpf, C. Schaller, “An Adaptive Level Set Method for Medical Image Segmentation,” In proceedings of the Annual Symposium on Information Processing in Meidcal Imaging, 2001.

[11] S. Ho, H. Cody, G. Greig, “ Snap: A Software Package for User-guided Geodesic Snake Segmentaion,” Tech. rep., University of North Caroline, Chapel Hill, April, 2003.

[12] A. Lefohn, J. Cates, R. Whitaker, “Interactive gpu-based level set for 3D Brain Tumor Segmentation,” Tech. rep. University of Utah, School of Computing Tech., April, 2003.

[13] M. Leventon, W. Grimson, O. Faugeras, “Statistical Shape Influence in Geodesic Active Contours,” In 5th IEEE EMBS International Summer School on Biomedical Imaging, pp. 8, June, 2002.

[14] V. Caselles, R. Kimmel, G. Sapiro, “Geodesic Active Contours,” In proceedings of IEEE International Conference on Computer vision, Boston, MA, pp. 694-699, 1995.

[15] V. Caselles, R. Kimmel, G. Sapiro, “Geodesic Active Contours,” International Journal of Computer Vision, vol. 22, pp. 61-79, no. 1, 1997.

[16] T. Chan and L. Vese, “Active Cotours Without Edges,” IEEE Transactions Image Processing, vol. 10, no. 2, pp. 266-277, Feb. 2001.

[17] N. Paraios and R. Deriche, “Geodesic Active Regions and Level Set Methods for Supervised Texture Segmentation,” Int. J. Comput. Vis., vol. 46, pp. 223-247, 2002.

[18] R. Ronfard, “Region-based strategies for Active Contour Models,” Int. J. Comput. Vis., vol. 13, pp. 229-251, 1994.

[19] C. Samson, L. Blanc-Feraud, G. Aubert, and J. Zerubia, “A Variational Model for Image Classification and Restoration,” IEEE Trans. Patt. Anal.

Mach. Intell., vol. 22, no. 5, pp. 460-472, May 2000.

[20] D. Mumford, J. Shah, “Optimal Approximation by Piecewise Smooth Function and Associated Variational Problems,” Communication on Pure and Applied Mathematics, vol. 42, pp. 577-685, 1989.

[21] S. Taheri, S. H. Ong, and V.F.H Chong, “Leve-set Segmentation of Brain Tumor using Threshold-based Speed Function,” Image and Vision Computing, vol. 28, pp. 26-37, 2010.

[22] J. Fang, Jie Yang, Z. Jia, and Nikola Kasabov, “Multilayer Level Set Method for Multiregion Image Segmentaion,” Optical Engineering, vol. 50 no. 6, pp. 607013-1-12, June 2011.

[23] Chunming Li, C. Y. Kao, John C. Gore and Zhaohua Ding, “Minimization of Region-Scalable Fitting Energy for Image Segmentaion,” IEEE Transactions. on Image Processing, vol. 17, no. 10, October 2008.

[24] Chunming Li, Rui Huang, Zhaohua Ding, J. Chris Gatenby, Dimitris N. Metaxas, and John C. Gore, “A Level Set Method for Image Segmentation in the Presence of Intensity Homogeneities with Application to MRI,” IEEE Transactions on Image Processing, vol. 20, no. 7, July 2011.

[25] Kaihua Zhang, Lei Zhang, Huihui Song, and Wengang Zhou, “ Active Contours with Selective Local or Global Segmentaion: A New Formulation and Level Set Method,” Image and Vision Computing, vol. 28, pp. 668-676, 2010.

[26] C. Y. Xu, A. Yezzi Jr., J. L. Prince, “On the Relationship Between Parametric and Geometric Active Contours.” In proceedings of 34th Asilomar Conference on Signals Systems and Computers, pp. 483-489, 2000.

[27] V. Caslles, F. Catte, T. Coll, and F. Dibos, “A Geometric Model for Active Contours in Image Processing,” Numer. Math., vol. 66, pp. 1-31, 1993

[28] R. Malladi, J.A. Sethian, and B.C. Vemuri, “ Shape Modeling with Front

Propagation: A Level Set Approach," IEEE Trans. Patt. Anal. Mach. Intell., vol. 17, pp. 158-175, 1995.

[29] S. Osher and R. Fedkiw, "Level Set Methods and Dynamic Implicit Surfaces," Applied Mathematical Science, Springer-Verlag NewYork, vol. 153, 2003.

[30] Y. Shi, W.C. Karl, "Real Time Tracking using Level Sets," IEEE Conference on Computer Vision and Pattern Recognition, vol. 2, pp. 34-41, 2005.

[31] P. Perona, J. Malik, "Scale-space and Edge Detection using Anisotropic Diffusion," IEEE Transaction on Pattern Analysis and Machine Intelligence, vol. 12, pp. 629-640, 1990.

List of Publications

Kiran Thapaliya and Kwon-Goo-Rak, "Splitting and Merging Algorithm Based on Local Statistics of Sub-Regions in Document Image," International Journal of KIMICS, Vol. 9, No.5, 487-490, Oct. 2011.

Kiran Thapaliya and Kwon-Goo-Rak, "An Efficient Extraction of Pulmonary Parenchyma in CT-Images using Connected Component Labeling," International Journal of Information and Communication Engineering, Vol. 9, No.6, Dec. 2011.

Kiran Thapaliya and Kwon-Goo-Rak, "Advanced Segmentation Using Bit-Plane Slicing Technique in Extraction of Lungs Region," In Proc. IEEE in Asian Himalayas International Conference on Internet AH-ICI 2011, Nov. 2011.

Kiran Thapaliya, Il-Cheol Park, and Goo-Rak Kwon, "Text Enhancement using Adaptive Thresholding," In Proc. of 5th Joint Conf. on Information and Communication Technology & 1st Yellow Sea Int. Conf. on Ubiquitous Computing, Aug. 2011.

Kiran Thapaliya and Kwon-Goo-Rak, "Extraction of Brain Tumor Based on Morphological Operations," 8th IEEE International Conference on Computing Technology and Information Management, April, 24-26, 2012.

Kiran Thapaliya and Goo-Rak Kwon, "An Advances Segmentation Using Area and Boundary Tracing Technique in Extraction of Lungs Region," Eurasip Journal in Image and Video Processing. (Submitted)

Kiran Thapaliya and Goo-Rak Kwon, "Automatic Segmentation of Pulmonary Parenchyma in CT-Images Using Centroid Value," Future Technology Research Association (FTRA). (Submitted)

Acknowledgement

The completion of this dissertation would not have been possible without the encouragement, help and friendship of many individuals. It is my privilege to thank the people who have supported and guided me throughout my pursuit of my MS course.

I would like to express my sincere gratitude and deep appreciation to my advisor, Prof. Goo-Rak Kwon for his guidance, encouragement and continuous support for this dissertation. Under his guidance, I have learnt to identify and approach research problems, and to develop and present the solutions in a comprehensible manner. His patient supervision and a sense of liberty that he granted to conduct my research studies would be treasured throughout my life.

I would also like to express my thankfulness to committee members, Prof. Jong `-An Park and Prof. Young-Suk Shin, for their, detail review, constructive criticism and insightful feedback during the preparation of this thesis.

During these years I have collaborated with many people. My sincere thank to all my lab mates of Digital Media Computing and all the friends for their cooperation and support during my MS course.

I am as ever, especially indebted to my parents and family for their love, support and encouragement in every step of my life. Their great understanding had made me to achieve my MS course.

Finally, the financial support of Global IT and Chosun University is greatly acknowledged.